

Influence of an Inclined Rock Stratum on In-Situ Stress State in an Open-Pit Mine

Wenhui Tan · P. H. S. W. Kulatilake ·
Hongbao Sun

Received: 29 August 2012 / Accepted: 23 August 2013 / Published online: 26 September 2013
© Springer Science+Business Media Dordrecht 2013

Abstract In-situ stress plays a major role with respect to deformation and stability around underground or surficial excavations located at significant depth. Many sedimentary rock masses are more or less horizontally bedded. However, a possibility exists to have one or few inclined rock strata such as dikes in these horizontally bedded formations. It is important to know how the in situ stress changes from a purely horizontally bedded situation to a horizontally bedded rock mass that contains one or few inclined rock strata. This paper presents such an investigation using the largest open-pit metal mine in China—as a case study. This mine has a bedded rock mass with one steeply inclined rock stratum. For the bedded rock mass, the vertical stress was calculated based on the overburden above each lithology. The available in situ stress measurements conducted at the mine were used to estimate the ratios of horizontal to vertical stress. Numerical modeling was performed for the two scenarios: (a) the horizontally bedded system subjected to both the in situ and boundary stresses and

(b) the mine lithological system that includes an inclined stiffer (denser) stratum intruding softer horizontally bedded system subjected to only boundary stresses to investigate the influence of an inclined rock stratum on the computed stress field. Thirty points were selected to compute the stresses on six planes of the inclined rock stratum. Due to the discontinuous nature of the geologic system at the interface between the stiffer inclined stratum and softer horizontally bedded system, one principal stress has become normal to the interface plane and the other two have become parallel to the interface plane with all three being perpendicular to each other. Presence of the stiffer inclined rock stratum has given rise to (a) increase in normal stresses up to about 120 % in the inclined rock stratum and (b) new shear stresses approximately in the range -10.0 to 15.0 MPa. This means, because most of the rock masses are not purely horizontally bedded, estimation of in situ stress through measurements as well as application of in situ stress in numerical modeling associated with underground or surficial excavations located at significant depth is a difficult exercise. A better way to estimate the in situ stresses for complex geologic systems may be through application of appropriate boundary stresses to the geologic system in a numerical model.

W. Tan · H. Sun
School of Civil and Environmental Engineering,
University of Science and Technology Beijing,
Beijing 100083, China

W. Tan · P. H. S. W. Kulatilake (✉)
Rock Mass Modeling and Computational Rock Mechanics
Laboratories, University of Arizona, Tucson, AZ 85721,
USA
e-mail: kulatila@u.arizona.edu

Keywords Inclined rock strata · In-situ stress ·
Normalized stress difference · Open-pit mine ·
3DEC

1 Introduction

In-situ stress plays a major role associated with deformation and stability of underground and deep surficial excavations in mining and civil engineering projects. Therefore, it is important to specify in situ stress accurately as an input parameter in performing numerical analyses of rock structures at significant depth. Ideally, the initial stress state of a problem domain should be decided based on field in situ stress measurements. To obtain accurate results for in situ stress through measurements, ideally the problem domain either should be homogeneous or horizontally layered with no inclined significant discontinuities. Unfortunately, for many problem domains, the in situ stress measurements are affected by the presence of either the complex, heterogeneous geology or significant inclined discontinuities close to the measurement points. The effect of fault geometry and fault geomechanical properties on in situ stress has been studied by some researchers through numerical modeling (Matsuki et al. 2009; Richard and Alan 2003; Shen et al. 2008; Su and Stephansson 1999; Su et al. 2003; Su 2004; Sun et al. 2008, 2009; Zang and Stephansson

2010; Wang et al. 2011; Stephansson and Zang 2012). However, the influence of inclined rock strata on in situ stress field has not been addressed in the literature. Intuitively, it is possible to expect a significant change of in situ stress arising due to presence of inclined rock strata. Stephansson and Zang (2012) provide a comprehensive review and some guidelines on estimating in situ stress under complicated subsurface conditions. They have specifically stated that numerical modeling can play a significant role in achieving the aforesaid task in addition to using the available data on in situ stress and analyzing the various in situ stress measurement data in an integrated fashion, which are obtained from field or laboratory tests.

In this paper, the influence of an inclined rock stratum on in situ stress is studied by conducting three dimensional numerical modeling for an open pit mine in China using the distinct element code 3DEC (Itasca 2007).

2 Mine Geology and the Scope of Study

Shuichang iron mine, located in Qianan district of Hebei Province, is the main supplier of iron ore for the

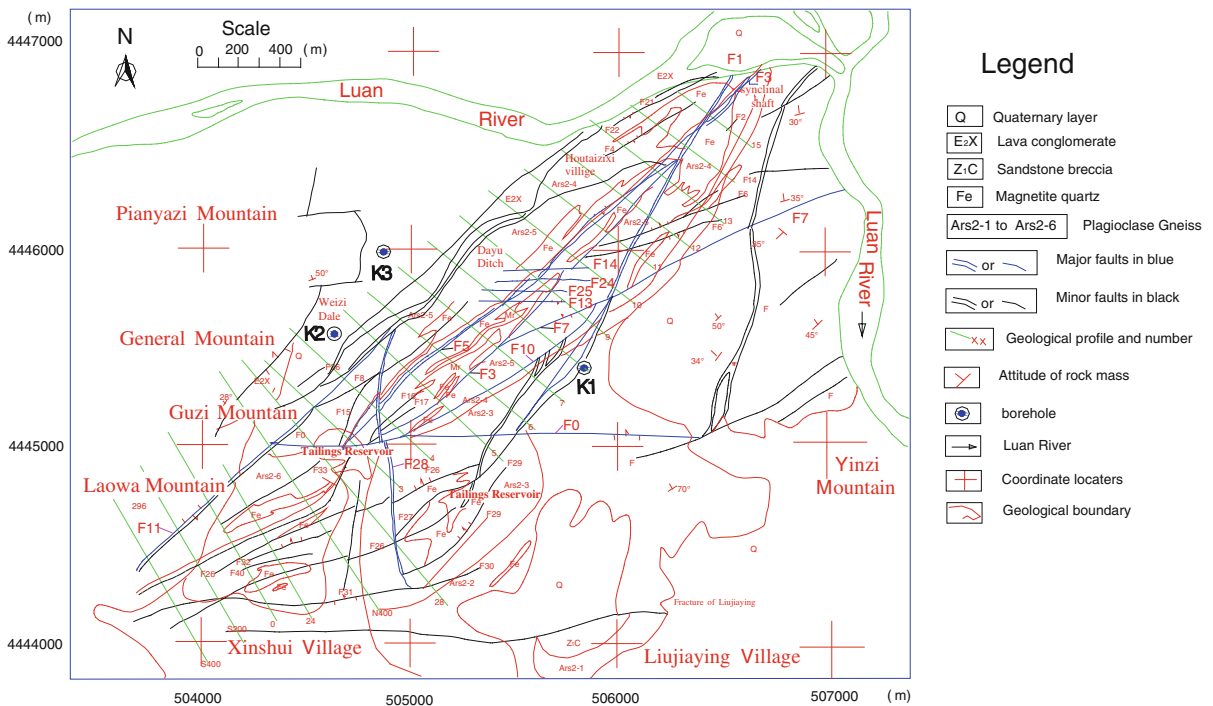


Fig. 1 Regional tectonic sketch of Shuichang open-pit mine

Capital Steel Corporation and also the largest open-pit metal mine in China. The pit is 2,900 m long and 1,000–1,400 m wide. According to the latest mining program of Shuichang iron mine, the height of the final slope of the mine is 760 m and the deep-concave mining depth is 540 m. For such a high slope, the effect of in situ stress on the slope cannot be ignored.

The rock mass of Shuichang iron mine is composed of different kinds of rock such as granite, gneiss, quartzite, conglomerate, pyroclastic rock, igneous rock and tectonite. The following layered system exists in the rock mass from the top to bottom: quaternary layer and artificial deposits, arkosic sandstone breccia and plagioclase gneiss. A steeply inclined magnetite quartz formation appears as an intrusion from the top to approximately 75 % of the whole depth. The quality of rock mass can be ranked as fair (Tan and Gao 2010). The iron ore body

(magnetite quartz) has a dip of approximately 70–80°SE and a strike of N 30°E. The Fault structures are very developed in the mine area and the regional tectonic sketch is shown in Fig. 1 according to the report of Geology Research Institute of the Capital Steel Corporation (2009). This paper addresses only the influence of the inclined magnetite quartz stratum on the in situ stress state; the effect of faults on the in situ stress will be addressed in a future paper.

3 In-Situ Stress Measurements and Estimation of In-Situ Stress Ratios

Because most of the deposits are subject to high geologic heterogeneity and significant tectonic movements during its geologic history, it is impossible to describe the distribution of the in situ stress in the rock

Table 1 Principal in situ stresses at different depths from Kaiser effect measurement on cores

Points	Depth (m)	Vertical principal stress, σ_v (MPa)	Max. horizontal principal stress, σ_H (MPa)	Min. horizontal principal stress, σ_h (MPa)	Direction of σ_H from North to East (°)	Direction of σ_h from North to West (°)
K1	110	3.06	5.64	4.11	84.60	5.40
	140	4.11	8.23	3.89	81.97	8.03
	200	5.36	10.22	4.72	81.98	8.02
	260	6.93	12.72	5.98	81.82	8.18
	310	8.22	16.35	8.01	82.37	7.63
	370	9.87	17.90	8.25	81.98	8.02
K3	160	4.11	7.18	4.34	83.91	6.09
	190	5.06	9.55	4.12	81.11	8.89
	250	6.85	11.95	6.65	82.95	7.05
	310	8.86	14.85	8.09	82.70	7.30
	370	9.78	18.26	10.08	82.60	7.40
	430	11.26	22.25	10.93	81.66	8.34
	490	12.81	24.25	12.34	83.03	6.97

Table 2 Results of hydraulic fracturing stress measurement in K2 borehole

No.	Depth at fracturing section (m)	Fracture parameters (MPa)						Stresses (MPa)			Fracture direction (°)
		P_b	P_r	P_s	P_H	P_0	T	σ_H	σ_h	σ_v	
1	265.2–265.8	9.11	6.59	5.96	2.60	2.01	2.52	9.28	5.96	7.02	N80°E
2	274.5–275.1	11.72	6.89	6.26	2.69	2.10	4.83	9.89	6.26	7.26	
3	302.4–303.0	11.78	8.42	8.00	2.96	2.38	3.36	13.21	8.00	8.00	

P_b : in situ fracture pressure; P_r : re-open fracture pressure; P_s : instant closing pressure; P_H : water column pressure of test section; P_0 : pore pressure of test section; T : tensile strength of rock mass; σ_H : max. horizontal principal stress; σ_h : min. horizontal principal stress; σ_v : vertical principal stress estimated by the thickness of rock layers

strata by a certain mathematical or physical model. Therefore, in situ stress measurements are usually performed to estimate the in situ stresses for the problem domain. The most widely used field in situ stress measurement methods are over-coring and hydraulic fracturing (Cai et al. 2000; Sjöberg et al. 2003; Zang and Stephansson 2010). The over-coring method releases the rock stresses around a borehole so that the complete stress tensor can then be determined from the resultant strains; the hydraulic fracturing method involves the pressurization of a borehole until failure occurs or pre-existing fractures are opened. Because the results of both these methods are affected by the geologic heterogeneities including the discontinuity system that exist around the in situ measurement points (IJRMMS 2003), tests on rock cores have been considered as an alternative approach, in particular the elastic strain recovery and the Kaiser Effect (Chen et al. 2006; Lehtonen et al. 2012). The basic principle of the Kaiser Effect is that acoustic emission of a loaded rock core occurs at the time when the stress exceeds the previously applied stress. The point on the stress–strain curve where emission starts or intensifies is called the Kaiser Effect point (Pollock 1989) and can be used to estimate the in situ stress. A digital acoustic emission system SAEU2S (USTB and CSC 2010) and a material testing machine have been used to conduct acoustic emission tests on core specimens taken from different depths of the boreholes K1 and K3 which are located in the middle region of the open-pit mine (Fig. 1). The test results, which are obtained from the report of University of Science and Technology Beijing and the Geology Research Institute of the Capital Steel Corporation (2009), are shown in Table 1. Also, the hydraulic fracturing stress measurements were conducted in the borehole K2 at three different depths. The results are given in Table 2.

Based on the aforementioned measurement results of 16 points, the linear regression models of the in situ stress state along the depth direction in the mine were estimated, and expressed in Fig. 2 and by the Eqs. (1)–(3) given below:

$$\begin{cases} \sigma_H = 0.0480D \quad (\text{MPa}) & (1) \\ \sigma_h = 0.0251D \quad (\text{MPa}) & (2) \\ \sigma_v = 0.0266D \quad (\text{MPa}) & (3) \end{cases}$$

In Eqs. (1)–(3), D is the depth in m, σ_H is the maximum principal in situ stress in the horizontal

direction, σ_h is the minimum principal in situ stress in the horizontal direction and σ_v is the intermediate principal in situ stress in the vertical direction. The direction of σ_H is 82.5 from North to East. From Eqs. (1)–(3), the ratios between the horizontal and vertical stresses are computed as $K_H = \sigma_H/\sigma_v = 1.80$ and $K_h = \sigma_h/\sigma_v = 0.94$. It is important to note that the measured in situ stresses vary spatially and are affected by the presence of the complex geology and the discontinuity network that exist in the geologic system. On the other hand, these estimated in situ stress ratios provide the mean best estimates from 16

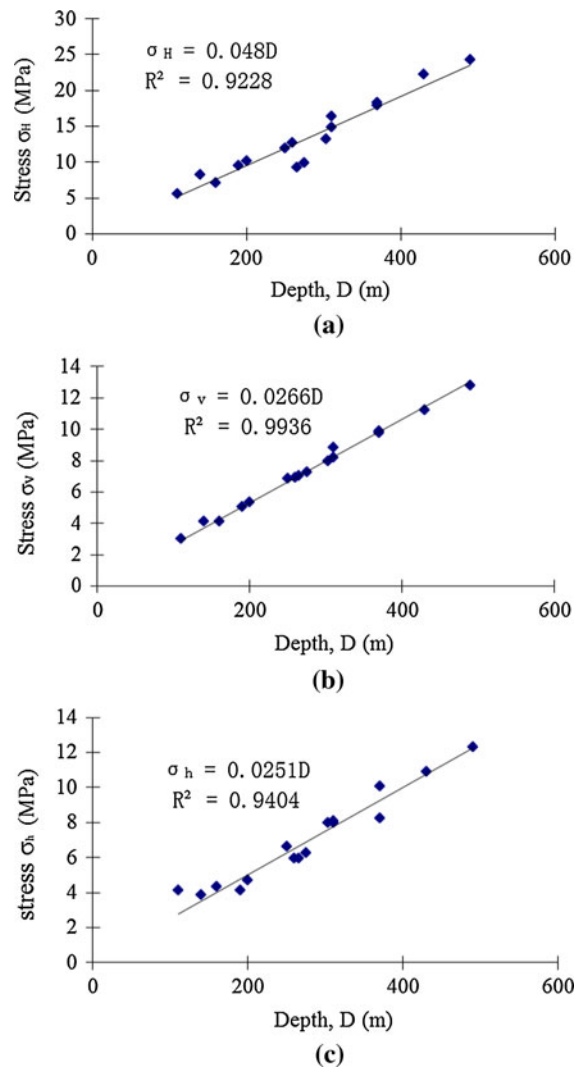


Fig. 2 Relations between in situ stresses and depth: **a** σ_H , **b** σ_v , **c** σ_h

Fig. 3 Lithological model used for computation.

- a** Three dimensional model,
- b** Section A–A (XZ plane),
- c** Section B–B (YZ plane)

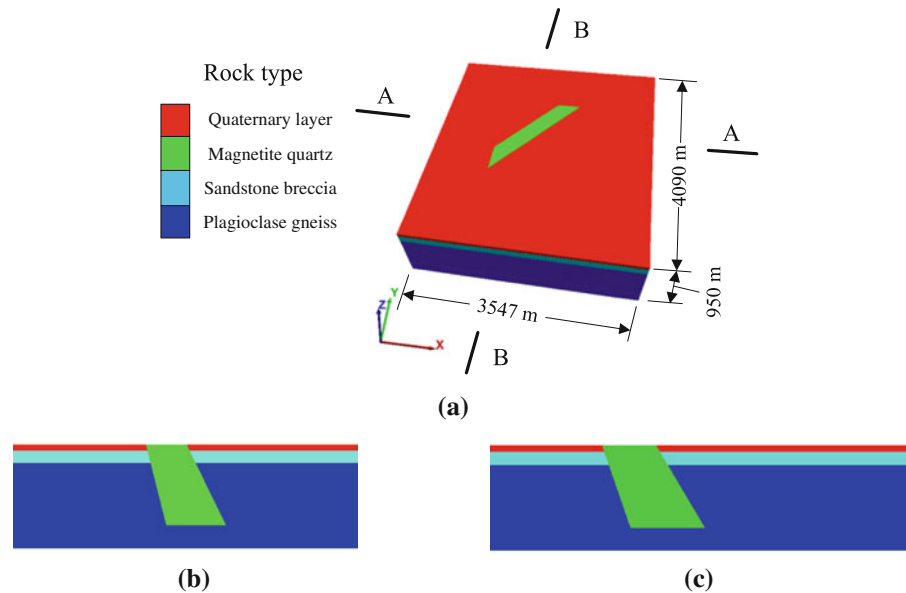


Table 3 Geometrical, physical and mechanical parameter values of different lithology

Lithology	Layer thickness (m)	Density, ρ (kg/m ³)	Bulk modulus, K (MPa)	Shear modulus, G (MPa)	Friction angle, φ (°)	Cohesion, c (MPa)	Tensile strength, σ_t (MPa)
Q	60	2,000	16.7	7.69	18	0.13	0.01
Z ₁ C	120	2,477	1,660	1,090	20	0.56	0.54
Ars2	770	2,630	2,260	1,620	35	2.99	0.82
Fe	Inclined	2,812	7,720	5,080	37	3.26	0.94

Q: quaternary layer and artificial deposits; Z₁C: sandstone breccia; Ars2: plagioclase gneiss; Fe: magnetite quartz

Table 4 Geomechanical parameter values used for the interfaces and joints

Interface position/ fictitious joint	Shear stiffness, JKS (Pa)	Normal stiffness, JKN (Pa)	Friction angle, φ (deg.)	Cohesion, C (MPa)	Tensile strength, σ_t (MPa)
Between Q and Z ₁ C	5.49e10	1.37e11	19.0	0.35	0.00
Between Z ₁ C and Ars	1.36e11	3.39e11	27.5	1.78	0.00
Between Ars and Fe	3.35e11	8.38e11	36.0	3.13	0.00
Between Q and Fe	2.54e11	6.36e11	27.5	1.70	0.00
Between Z ₁ C and Fe	3.09e11	7.71e11	28.5	1.91	0.00
Fictitious joint in Ars	1.62e11	4.05e11	35.0	2.99	0.82

in situ stress measurements obtained from different locations in the considered site. Extremely high obtained correlation coefficient, R , values indicate that the obtained linear regression models are excellent. Therefore, it is reasonable to use these in situ stress ratios to apply boundary and in situ stress conditions for the different geological units that exist in the computational model domain.

4 Numerical Modeling

4.1 Setting Up of the Numerical Model

To study the influence of the inclined rock stratum on in situ stress distribution, a geomechanical model of the mine was built based on the results obtained from engineering geology investigation and rock testing.

The selected model region is 4,090 m long, 3,547 m wide and 950 m high, as shown in Fig. 3. The directions of the maximum horizontal principal stress, minimum horizontal principal stress and the intermediate vertical principal stress are set along the X, Y and Z coordinate directions of 3DEC, respectively (Fig. 3). The linear elastic-perfect plastic constitutive model is used to represent the material behavior of each lithology in the computational model. The Mohr–Coulomb model is selected to represent the rock strength of each lithology. Geometrical, physical and mechanical parameter values used to represent different lithology are given in Table 3 (Cai et al. 2011).

Coulomb slip model is used to represent interface or fictitious joint strength in the model region. The

interfaces are used between the different lithology and the fictitious joints (that behave as intact rock) are used in the Ars2 lithology to create polyhedra in the problem domain to perform 3DEC analysis (Kulatilake et al. 1992). For both the fictitious joints and interfaces, the geomechanical parameters are estimated according to the procedure given in Kulatilake et al. (1992). The values of Joint Shear Stiffness, JKS, and Joint Normal Stiffness, JKN, are estimated according to the relations shear modulus (G)/ $JKS = 0.008–0.012$ m and $JKN/JKS = 2–3$. For fictitious joints, the intact rock G value is substituted in using the aforementioned relations. For interfaces, the average G value of the two layers is used in using the aforementioned relations. The geomechanical

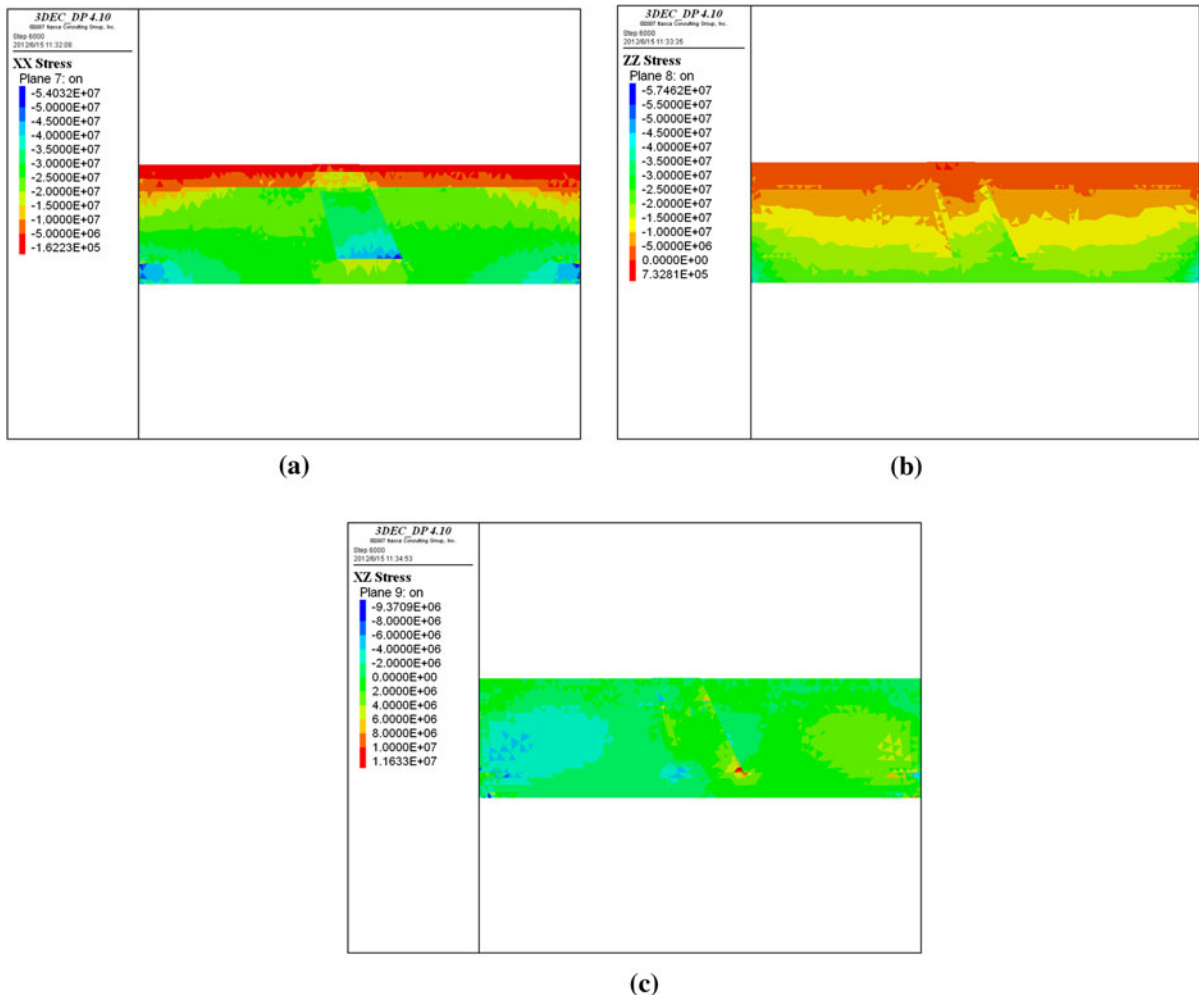


Fig. 4 Stress distribution on XZ plane resulted from Scenario ②. **a** SXX, **b** SZZ, **c** SXZ

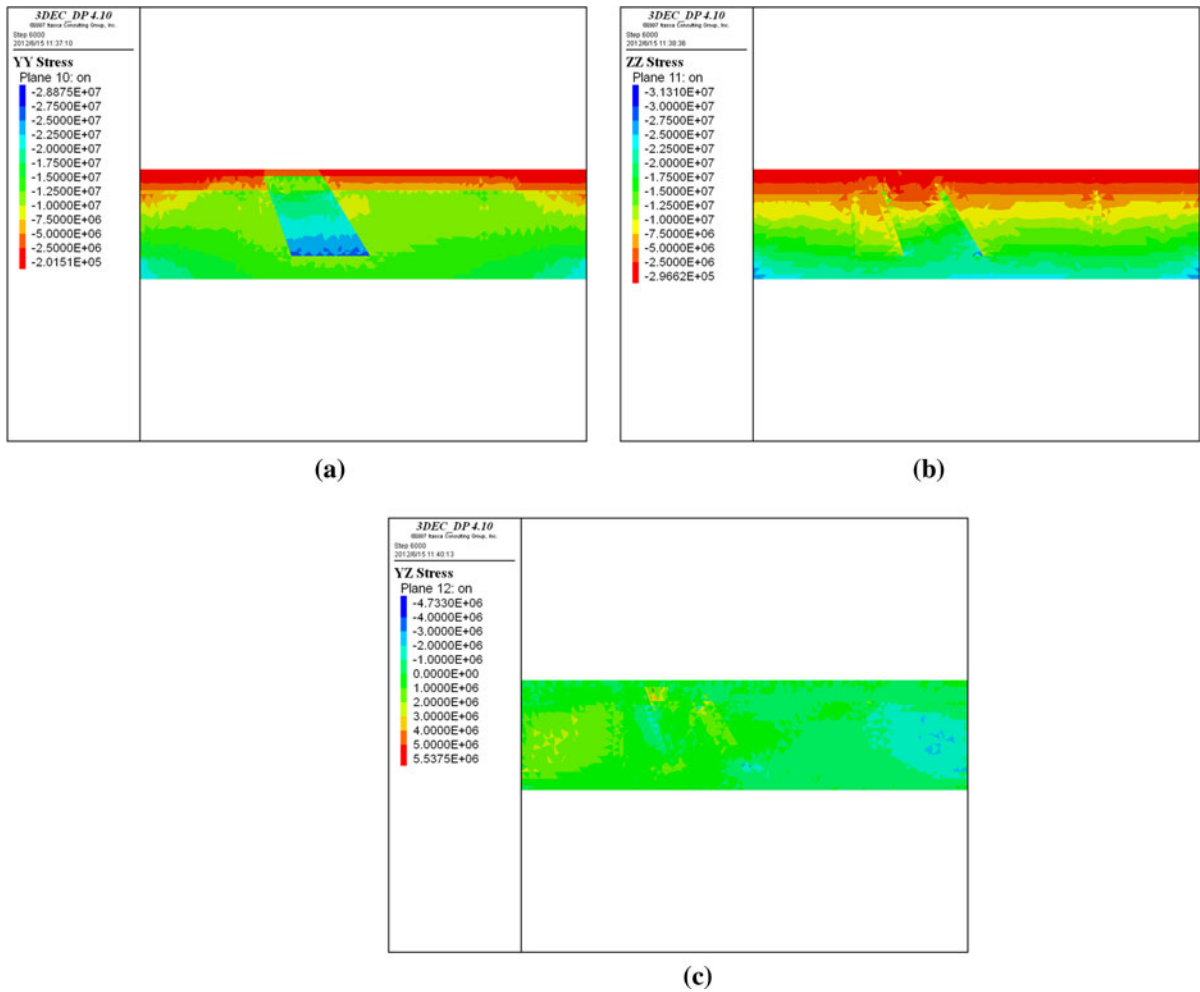


Fig. 5 Stress distribution on YZ plane resulted from Scenario ②. **a** SYY, **b** SZZ, **c** SYZ

parameter values used for the fictitious joints and the interfaces are given in Table 4.

For the horizontally bedded lithology, identified as Scenario ① in the next section, the vertical in situ stress was calculated for each rock layer using the known overburden above it; the two horizontal in situ stresses were calculated by multiplying the calculated vertical in situ stress by the ratios of horizontal to vertical stress computed in the previous section. The boundary stresses to be applied on the four lateral boundaries for the model region were calculated using the same concepts as for the in situ stress. At the top boundary of the model region, all the stresses were set to zero. Along the bottom boundary, the velocity in the Z direction was set to zero.

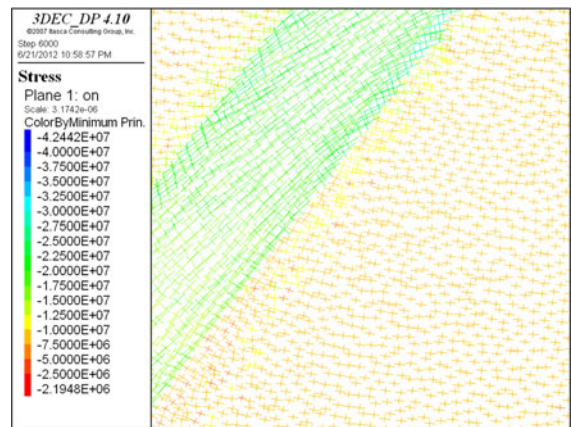


Fig. 6 Principal stress vectors in and around the Fe stratum on the horizontal plane at the depth of 150 m from the top (in the Z₁C layer)

4.2 Influence of the Inclined Rock Stratum on In-Situ Stress State

For a layered deposit having horizontal strata, the in situ stresses are equal to the boundary stresses in respective directions, and vary only along the depth direction and they can be calculated analytically. This scenario termed as Scenario ① can be simulated in the computational model to check whether the numerical model is set up correctly. In the numerical model, Scenario ① can be simulated either by applying the in situ stresses or the boundary stresses or both. The computational time for Scenario ① can be minimized by applying both the in situ stresses and the boundary stresses. If this horizontally bedded system is intruded by an inclined stratum (this system is identified as Scenario ② in the paper), then it is not possible to calculate the in situ stresses throughout the computational domain analytically. However, in situ stresses for Scenario ② can be calculated by applying appropriate boundary stresses to the computational model which includes the inclined stratum with the bedded system. If the boundaries are selected quite far away from the inclined stratum, then it is reasonable to apply the same boundary stresses as for the aforementioned horizontally bedded system to study the effect of the inclined stratum on in situ stresses. Thus, to investigate the influence of the inclined rock stratum on the stress state throughout the computational domain, two scenarios were set up as follows: Scenario ①: application of the in situ stresses and the boundary stresses only for the horizontally bedded system (that means without the inclined Fe stratum) that exists at the mine; Scenario ②: application of only the boundary stresses to the lithological system that consists of the aforementioned horizontally bedded system with the intruded inclined FE stratum. Note that the density, gravitational acceleration and geomechanical properties are specified for each stratum. Discontinuity mechanical properties are assigned for the interfaces between different strata. Also note that the same boundary stresses were applied to both Scenarios ① and ②. Computation of these boundary stresses were discussed earlier in paragraph 3 of Sect. 4.1. Under these conditions all the stress values in the system can be calculated for Scenario ②. These stresses can be compared with the stresses resulting from Scenario ① to evaluate the effect of stiffer inclined stratum on the in situ stress.

In Scenario ①, because the Fe stratum does not exist, the geologic system is a horizontally layered system. Since the in situ stress was also applied in addition to the boundary stresses, the equilibrium condition was reached quickly and the stresses matched very well with the intuition. S_{XX} (normal stress in the X direction), S_{YY} (normal stress in the Y direction), S_{ZZ} (normal stress in the Z direction) values changed gradually with depth as expected for a layered system. The shear stresses S_{XZ} and S_{YZ} were found to be equal to zero or almost zero as expected.

In Scenario ②, the inclined stratum of Fe is included along with the lateral stress boundary conditions. The unit weight of Fe stratum is significantly higher compared to the rest of the lithology present in the model region. In addition, the Fe stratum is a steeply inclined intrusion cutting the rest of the lithology. S_{XX} , S_{ZZ} and S_{YY} values are significantly higher in the Fe stratum compared to that of the bedded rocks at the same depth (Figs. 4a, b, 5a, b). Note that for the horizontally bedded system without the FE stratum, the S_{XX} , S_{ZZ} and S_{YY} change

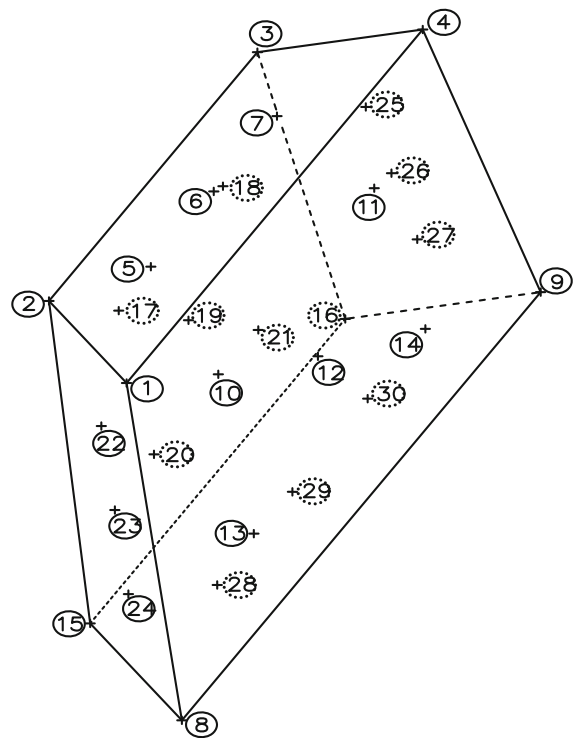


Fig. 7 Points selected on the six planes of the Fe block for stress calculation (*dotted lines* and points are on invisible planes; *solid lines* and points are on visible planes)

Table 5 X–Y–Z coordinate values of the selected points on the Fe block surface

No.	X	Y	Z	No.	X	Y	Z
①	– 773.45	– 618.82	750	⑩	326.38	1044.88	0
②	– 773.45	– 126.12	750	⑪	– 517.12	142.36	562.5
③	125.41	1044.88	750	⑫	– 67.68	727.86	562.5
④	503.61	1044.88	750	⑬	– 260.78	410.84	375
⑤	– 501.46	– 18.04	750	⑭	– 453.88	93.82	187.5
⑥	– 229.47	336.27	750	⑮	– 4.44	679.32	187.5
⑦	42.52	690.58	750	⑯	– 773.45	– 458.43	562.5
⑧	– 773.45	– 970.36	0	⑰	– 773.45	– 544.51	375
⑨	773.45	1044.88	0	⑱	– 773.45	– 630.59	187.5
⑩	– 437.32	– 268.81	562.5	⑲	373.37	1044.88	562.5
⑪	234.94	606.98	562.5	⑳	432.22	1044.88	375
⑫	– 67.46	125.15	375	㉑	491.08	1044.88	187.5
⑬	– 403.59	– 406.63	187.5	㉒	– 442.61	– 276.27	0
⑭	336.13	563.04	187.5	㉓	– 111.77	164.12	0
⑮	– 773.45	– 387.94	0	㉔	219.07	604.51	0

gradually with Z, but remain the same for all X and Y values at the same depth. Figures 4 and 5 show drastic changes of SXX, SYY and SZZ close to the interfaces between FE block and layered geologic material. Figures 4c and 5c show existence of high SXZ and SYZ, respectively on the interfaces between the Fe stratum and the rest of the layered lithology and also at some other locations in the model region. Note that for the horizontally bedded system without the FE stratum, the shear stresses SXZ and SYZ are zero throughout the model region. Figure 6 shows how the principal stress vector directions change from the model boundary to the interface between the Fe stratum and Z₁C layer on the horizontal plane at the depth of 150 m from the top. Due to the discontinuous nature of the geologic system at the interface elements, one principal stress is normal to the interface plane and the other two are parallel to the interface plane and they are perpendicular to each other. Also, at the interfaces, the material properties change significantly across each interface from stiff FE material to a softer geologic material through an interface material which

has in between material properties of the said two geologic materials. Under such a composite material situation, high stress magnitudes should occur in the stiffer material. At the model boundaries the principal stresses are parallel to X, Y and Z directions. Figure 6 shows the aforesaid expected change of stress directions and magnitudes at the interfaces and indicates clearly the effect of the inclined rock stratum on the in situ stress system.

The aforementioned example clearly shows that inclined geologic intrusions can change the in situ stress state significantly. Estimation of such in situ stress requires application of numerical modeling similar to the Scenario ② case as shown above.

4.3 Spatial Variation of Stress on the Six Planes of the Inclined Fe Rock Stratum

Thirty locations were selected on the six planes of the Fe block (Fig. 7) to investigate how the stress changes on the interfaces between the Fe block and the rest of the horizontally layered lithology of the geologic

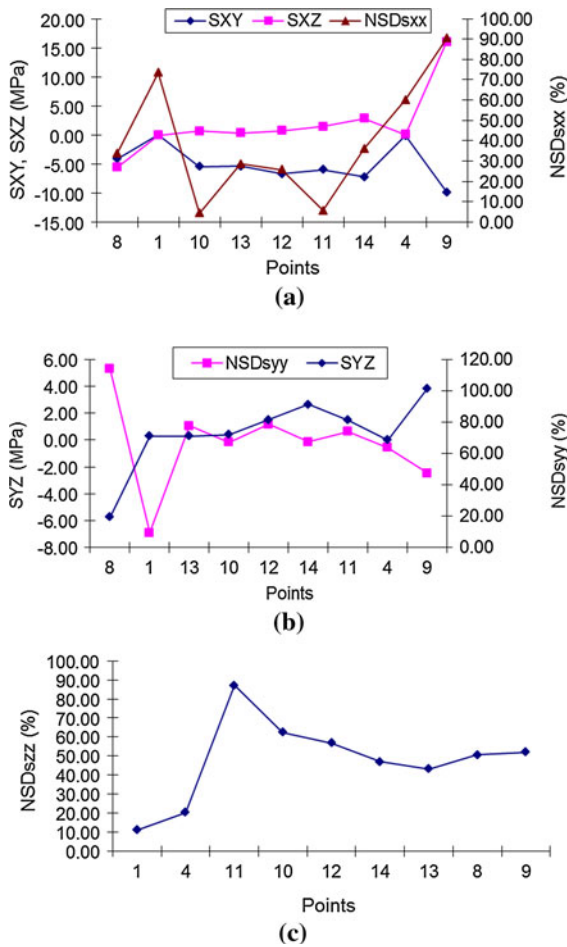


Fig. 8 Variation of stress on the right plane (1–4–8–9) of the Fe block. **a** X direction, **b** Y direction, **c** Z direction

system. Table 5 provides the X–Y–Z coordinates of the selected locations. A term called Normalized Stress Difference (NSD) is defined as given in Eqs. 4–6 given below to show the effect of the Fe block on the normal stresses act along the directions X, Y and Z at the selected locations.

$$\begin{cases} NSD_{SXX} = \frac{SXX_{Fe} - SXX_{No\ Fe}}{SXX_{No\ Fe}} \times 100 \% & (4) \\ NSD_{SYY} = \frac{SYY_{Fe} - SYY_{No\ Fe}}{SYY_{No\ Fe}} \times 100 \% & (5) \\ NSD_{SZZ} = \frac{SZZ_{Fe} - SZZ_{No\ Fe}}{SZZ_{No\ Fe}} \times 100 \% & (6) \end{cases}$$

In Eqs. 4–6, SXX_{Fe} , SYY_{Fe} and SZZ_{Fe} are the stresses along the three directions X, Y and Z, respectively, calculated in Scenario ②; $SXX_{No\ Fe}$, $SYY_{No\ Fe}$, $SZZ_{No\ Fe}$ are the same stresses calculated in Scenario ①. For Scenario ①, theoretically, the shear

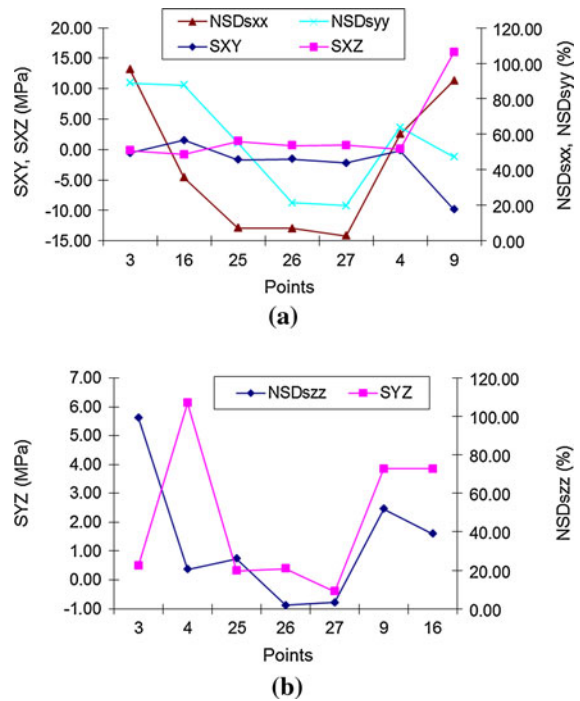


Fig. 9 Variation of stress on the back plane (3–4–9–16) of the Fe block. **a** X direction, **b** Z direction

stresses are zero. Therefore, the influence of Fe block on the shear stresses can be evaluated by directly using the shear stress values resulted from Scenario ②.

Figures 8, 9 and 10 show the obtained stresses on the right, back and bottom planes of the FE block. The order of the points shown in each figure is either according to increasing X coordinate values (in the X direction), or Y coordinate values (in the Y direction) or Z coordinate values (in the Z direction). The plane shown in Fig. 9 is parallel to the X axis; so there is no Y direction figure. The accuracy of the calculated values increases with decreasing element size. Unfortunately, the computational time increases with decreasing element size. To compromise between the accuracy and computational time, 60 m was used as the element size in discretizing each lithology in the numerical model. Therefore, it is important to note that the values shown in Figs. 8, 9 and 10 are not exactly on the boundaries of the Fe block; these values are coming from the closest element centers to the boundary of the Fe block.

Note that without the Fe block, all the normal stresses are exactly zero at the very top surface of the Fe block. At the element centers which are closest to

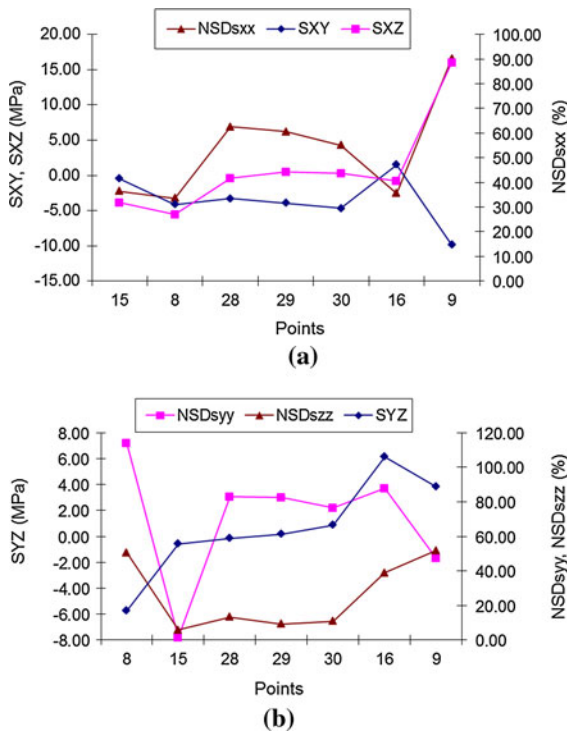


Fig. 10 Variation of stress on the bottom plane (8–9–15–16) of the Fe block. **a** X direction, **b** Y direction

the very top surface, the normal stresses are close to zero even though they are not exactly zero; these close to zero normal stresses are used in computing the normalized stresses at the top surface of the Fe block. This is the reason why in Figs. 8, 9 and 10, for some points which lie on the top surface of the Fe block, close to 100 % change have been obtained for certain normal stresses. Highest normal stresses also can be seen at the corner points of the bottom surface of FE block. Note that the interface elements are used between the boundaries of the FE block and the horizontally layered material. This means material properties change significantly from a stronger FE block to a weaker layered rock through an interface material which has in between material properties in crossing the interfaces. Under such a composite material situation, high stress magnitudes should occur in the stiffer material. Also note that large displacements are allowed at the interfaces. In addition, the highest discontinuous situation exists at these corner points. Therefore, the displacements and

stresses can be highly discontinuous at these corner points. If the points located at the top surface of the Fe block are ignored, it can be stated that the presence of the Fe block has given rise to change in normal stresses up to about 120 %. Shear stresses approximately in the range -10.0 to 15.0 MPa have resulted due to the presence of the Fe block (see Figs. 8, 9, 10); the highest shear stresses appear at the corner points of the Fe block. These findings clearly show that the presence of the Fe block has changed the in situ stress system significantly.

5 Conclusions

The measured in situ stress data resulted in the following estimations for the two principal stress ratios: $k_H = 1.80$ and $k_h = 0.94$. In-situ stress system can significantly change between a geological system that has horizontally bedded strata and a system that includes an inclined intrusion cutting the aforesaid horizontally bedded system. Due to the discontinuous nature of the geologic system at the interface between the stiffer inclined stratum and softer horizontally bedded system, one principal stress has become normal to the interface plane and the other two have become parallel to the interface plane with all three being perpendicular to each other. Presence of the stiffer inclined rock stratum has given rise to (a) increase in normal stresses up to about 120 % in the inclined rock stratum and (b) new shear stresses approximately in the range -10.0 to 15.0 MPa. This means, one should not apply the in situ stresses applicable for a purely horizontally bedded rock mass to a horizontally bedded rock mass having at least one significant inclined stratum in performing stability computations associated with underground or surficial excavations located at significant depth. A better way to estimate the in situ stresses for complex geologic systems may be through application of appropriate boundary stresses to the geologic system in a numerical model as done in this study.

Acknowledgments This work was financially supported by the key project of National Natural Science Foundation of China (Number: 51034001). The first author of the paper is grateful to the Chinese Scholarship Council for providing a scholarship to conduct the research described in this paper as a Visiting Research Scholar at the University of Arizona, USA.

References

- Cai MF, Qiao L, Li HB (2000) Principle and technique of in situ stress measurement. Science Press, Beijing
- Cai MF, Qiao L, Li CH, Wang JA (2004) In-situ stress measurement with hydraulic fracturing technique in deep slope rock mass of Shuichang iron mine. *Min Res Dev* 24(4): 11–13
- Cai MF, Xie MW, Wang, JA, Li CH, Qiao L, Tan WH (2011) Stability analysis and optimum design of high and steep slope in a deep-concave open-pit mine. In: Cai MF (ed) *Rock mechanics: achievements and ambitions—proceedings of the 2nd ISRM international young scholars' symposium on rock mechanics*. Beijing, Balkema, London, pp 581–585
- Chen Q, Zhu BL, Hu HT (2006) Experimental research on measurement of in situ stress field by Kaiser effect. *Chin J Rock Mech Eng* 25(7):370–376
- Geology Research Institute of the Capital Steel Corporation (2009) Supplement exploration and geological report of Shuichang iron mine for revised design. Report, Beijing
- IJRMMS (2003) Special issue on rock stress estimation: ISRM Suggested Methods and associated supporting papers. *Int J Rock Mech Min Sci* 40:955–1025
- Itasca Consulting Group, Inc (2007) 3DEC-Three dimensional distinct element code, version 4.1. Minneapolis
- Kulatilake PHSW, Ucpirti H, Wang S, Radberg G, Stephansson O (1992) Use of the distinct element method to perform stress analysis in rock with non-persistent joints and to study the effect of joint geometry parameters on the strength and deformability of rock masses. *Rock Mech Rock Eng* 25(4):253–274
- Lehtonen A, Cosgrove JW, Hudson JA, Johansson E (2012) An examination of in situ rock stress estimation using the Kaiser effect. *Eng Geol* 124:24–37
- Matsuki K, Nakama S, Sato T (2009) Estimation of regional stress by FEM for a heterogeneous rock mass with a large fault. *Int J Rock Mech Min Sci* 46(1):31–50
- Pollock A (1989) Acoustic emission inspection, 9th edn, vol 17. *Metals Handbook*, ASM International (reprint.), Novelty
- Richard JN, Alan FC (2003) Very high strains recorded in mylonites along the alpine fault, New Zealand: implications for the deep structure of plate boundary faults. *J Struct Geol* 25(12):2141–2157
- Shen HC, Cheng YF, Zhao YZ, Zhang JG, Xia YB (2008) Study on influence of faults on geostress by measurement data and numerical simulation. *Chin J Rock Mech Eng* 27(Suppl):3985–3990
- Sjöberg J, Christiansson R, Hudson JA (2003) ISRM Suggested Methods for rock stress estimation—part 2: overcoring methods. *Int J Rock Mech Min Sci* 40:999–1010
- Stephansson O, Zang A (2012) ISRM suggested methods for rock stress estimation—part 5: establishing a model for the in situ stress at a given site. *Rock Mech Rock Eng* 45:955–969
- Su SR (2004) Effect of fractures on in situ rock stresses studied by the distinct element method. *Int J Rock Mech Min Sci* 41(1):159–164
- Su SR, Stephansson O (1999) Effect of a fault on in situ stress studied by distinct element method. *Int J Rock Mech Min Sci* 36(8):1051–1056
- Su SR, Zhu HH, Wang ST, Stephansson O (2003) Effect of physical and mechanical properties of rocks on stress field in the vicinity of fractures. *Chin J Rock Mech Eng* 22(3):370–377
- Sun WC, Min H, Wang CY (2008) Three dimensional geostress measurement and geomechanical analysis. *Chin J Rock Mech Eng* 27(Suppl):3778–3785
- Sun LJ, Zhu YQ, Yang GL, Yin JY (2009) Numerical simulation of ground stress field at ends and vicinity of a fault. *J Geod Geodyn* 29(2):7–12
- Tan WH, Gao DQ (2010) Comprehensive Evaluation on Mechanical Environment of Rockmass in High-steep Slopes. In: Jiang MJ, Liu F, Botton M (eds) *Proceedings of an international symposium geomechanical geotechnical: from micro to macro*, October 10–13, 2010, Shanghai, China. Balkema, London, pp 1109–1114
- University of Science and Technology Beijing (USTB), the Capital Steel Corporation (CSC) (2010) Investigation on slope stability of revised design of Shuichang iron mine of Capital Steel Corporation Report. University of Science and Technology Beijing
- Wang YX, Deng GZ, Cao J (2011) Numerical simulation of fault-zone's influence on stress in deep mine. *J Xi'an Univ Sci Tech* 31(6):818–822
- Zang A, Stephansson O (2010) *Stress field of the earth's crust*. Springer, New York